

# Critical surface tension of poly(vinylidene fluoride-co-hexafluoroacetone) by the contact angle method

Yoshihasa Kano

Research Laboratory, LINTEC Corporation, 5-14-42, Nishiki-cho, Warabi-shi, Saitama 335, Japan

and Saburo Akiyama

Laboratory of Chemistry, Faculty of General Education, Tokyo University of Agriculture and Technology, 3-5-8, Saiwai-cho, Fuchu-shi, Tokyo 183, Japan

(Received 7 January 1991; revised 25 April 1991; accepted 7 May 1991)

The contact angles  $\theta$  of dispersion (D), polar (P) and hydrogen bonding (H) liquids on poly(vinylidene fluoride-co-hexafluoroacetone) (P(VDF-HFA); HFA content 6.5, 8.3 and 10.4 mol%) were measured. The critical surface tensions  $\gamma_c$  of P(VDF-HFA) were evaluated by the Zisman plot ( $\cos \theta$  versus  $\gamma_L$ ), Young-Dupre-Good-Girifalco plot ( $1 + \cos \theta$  versus  $1/\gamma_L^{0.5}$ ) and the  $\log(1 + \cos \theta)$  versus  $\log(\gamma_L)$  plot. The following results were obtained: the  $\gamma_c$  values of P(VDF-HFA) evaluated for the P liquids were larger than those for the D and H liquids; the  $\gamma_c$  values estimated by the Zisman plot were smaller than those obtained by the other plots; the surface tension  $\gamma_s$  values of P(VDF-HFA) revealed a minimum at the HFA content of 8.3 mol%. It was expected that P(VDF-HFA) with HFA = 8.3 mol% induced surface segregation most easily.

(Keywords: P(VDF-HFA); Zisman plot; Young-Dupre-Good-Girifalco plot; critical surface tension; surface segregation)

## INTRODUCTION

Poly(vinylidene fluoride-co-hexafluoroacetone), P(VDF-HFA), possesses excellent properties of resistance to heating, weather and chemicals, water repellency and non-tackiness. Recent studies have investigated the miscibility of P(VDF-HFA) with poly(methyl methacrylate) (PMMA)<sup>1</sup>, poly(ethylene-co-vinyl acetate) (EVAc)<sup>2</sup> and poly(carbonate) (PC)<sup>3</sup>.

The surface properties (water repellency, non-tackiness) of P(VDF-HFA) are closely related to the surface tension  $\gamma_s$ . Estimation of  $\gamma_s$  of the polymer solid has generally been made by the contact angle method<sup>4-11</sup>. Zisman<sup>4,5</sup> measured the contact angles  $\theta$  of organic liquids on various polymer solids. He found that the relationship between  $\cos \theta$  and the surface tension of liquid  $\gamma_L$  gave rise to a good straight line. He named the critical surface tension  $\gamma_c$ , which was the value of  $\gamma_L$  at  $\cos \theta = 1$  by extrapolating the straight line.

Good and Girifalco<sup>6</sup> defined the interaction parameter  $\Phi_G$  using the work of adhesion  $W_a$  and the work of cohesion  $W_c$ :

$$\Phi_G = W_a / (W_{c1} W_{c2})^{0.5} \quad (1)$$

They presented the following equation:

$$W_a = 2\Phi_G (\gamma_s \gamma_L)^{0.5} \quad (2)$$

Using equation (2) and Young-Dupre's equation

$$W_a = \gamma_L (1 + \cos \theta) \quad (3)$$

the equation of Young-Dupre-Good-Girifalco was expressed as:

$$1 + \cos \theta = 2\Phi_G (\gamma_s / \gamma_L)^{0.5} \quad (4)$$

Good and Girifalco<sup>6</sup> measured the contact angles  $\theta$  of poly(tetrafluoroethylene) (PTFE) with organic liquids. They evaluated the  $\Phi_G$  and the  $\gamma_s$  by use of the  $1 + \cos \theta$  versus  $1/\gamma_L^{0.5}$  plot. However, we<sup>7-11</sup> have found that the  $\gamma_s$  values of various polymers can be estimated by the  $\log(1 + \cos \theta)$  versus  $\log(\gamma_L)$  plot.

We investigated the miscibility, adhesive properties, viscoelastic properties and surface structure for poly(2-ethyl hexyl acrylate-co-acrylic acid-co-vinyl acetate) (PEHA/P(VDF-HFA)) blends<sup>12-18</sup>. The following results were obtained. It was confirmed that PEHA and P(VDF-HFA) were enriched at the interface of blend and substrate and at the surface of blends, respectively, in blends with the P(VDF-HFA) component over 50 wt% by the ATR-FTi.r. method (Figure 1)<sup>15</sup>.  $I_{870}$  is the C-F absorbance for P(VDF-HFA) at  $870 \text{ cm}^{-1}$  and  $I_{1730}$  is the C=O absorbance for PEHA at  $1730 \text{ cm}^{-1}$ . It was suggested that the surface segregation<sup>19,20</sup> of the low surface energy component (P(VDF-HFA)) occurred on the surface of the blend in contact with air<sup>18</sup>.

In the present paper, the contact angles  $\theta$  of P(VDF-HFA) (with HFA content of 6.5, 8.3 and 10.4 mol%) with dispersion (D), polar (P) and hydrogen bonding (H) liquids were measured. The critical surface

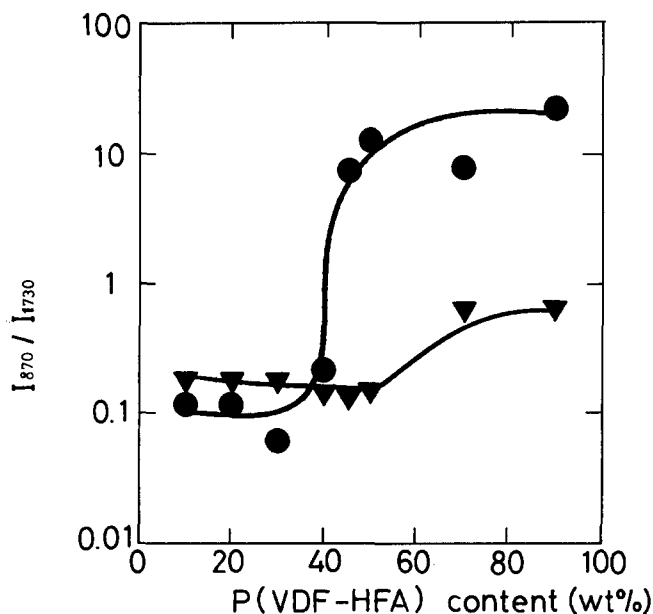


**Figure 1** Variation of absorbance ratio of PEHA/P(VDF-HFA) blends. ●, Surface of blends; ▼, interface of blends and substrate

tensions  $\gamma_c$  of P(VDF-HFA) were estimated by the Zisman plot ( $\cos \theta$  versus  $\gamma_L$ ), the Young–Dupre–Good–Girifalco plot ( $1 + \cos \theta$  versus  $1/\gamma_L^{0.5}$ ) and the  $\log(1 + \cos \theta)$  versus  $\log(\gamma_L)$  plot<sup>7–11</sup>. The surface segregation for the PEHA/P(VDF-HFA) blends was investigated with  $\gamma_s$ .

## THEORETICAL BACKGROUND

### Young–Dupre–Good–Girifalco plot

The  $1 + \cos \theta$  versus  $1/\gamma_L^{0.5}$  plot obtained by the contact angles  $\theta$  of homogeneous liquids on a polymer solid gives rise to a good straight line with the experimental data. However, in many cases the straight line greatly deviated from the origin with the polarity of the liquids<sup>11</sup>. In such cases, the straight line can be expressed as:

$$1 + \cos \theta = \lambda \gamma_L^{-0.5} + \phi \quad (5)$$

where  $\lambda$  and  $\phi$  are the slope and the intercept of  $1 + \cos \theta$  at  $1/\gamma_L^{0.5} = 0$  in the  $1 + \cos \theta$  versus  $1/\gamma_L^{0.5}$  plot, respectively. These parameters are constant with homogeneous liquids. The critical surface tension  $\gamma_c$  is defined as the value of  $\gamma_L$  at  $\theta \rightarrow 0$ . The relationship between  $\lambda$  and  $\phi$  is expressed in the following equation by the use of  $\gamma_c$ :

$$\lambda = (2 - \phi)\gamma_c^{0.5} \quad (6)$$

$$\lambda < 0, \quad \phi < 2 \quad \text{for } d \cos \theta / d\gamma_L < 0 \quad (6a)$$

Using equation (5), Young–Dupre’s equation (3) and Good–Girifalco’s equation (2), and neglecting the spreading pressure  $\pi_c$ , the Good–Girifalco interaction parameter  $\Phi_G$  is expressed as:

$$\Phi_G = (1/2\gamma_s^{0.5})[(2 - \phi)\gamma_c^{0.5} + \phi\gamma_L^{0.5}] \quad (7)$$

where  $\gamma_s$  is the surface tension of solid. The parameter  $\Phi_G^0$ , defined as  $\Phi_G$  at  $\theta \rightarrow 0$ , is expressed as follows:

$$\Phi_G^0 = (\gamma_c/\gamma_s)^{1/2} \quad (8)$$

### The $\log(1 + \cos \theta)$ versus $\log(\gamma_L)$ plot

As the interaction between liquid and solid is approximated by use of the geometric mean law,  $\Phi_0$  is defined as the indication of polarity in  $\Phi_G$ . Furthermore, we also took account of an adjustable parameter ( $X_{LS}$ ) within  $\Phi_G$  as a departure from the interaction estimated by the geometric law<sup>11</sup>. Thus,  $\Phi_G$  is expressed as:

$$\begin{aligned} \Phi_G &= (X_L^d X_s^d)^{0.5} + (X_L^p X_s^p)^{0.5} + X_{LS} \\ &= \Phi_0 + X_{LS} \end{aligned} \quad (9)$$

where  $X_j^d$  and  $X_j^p$  are the dispersion and the polarity of the  $j$  component.

Wu<sup>21</sup> reported that the polarity  $X_j^p$  was estimated with the solubility parameter  $\delta$  and the polarity component of solubility parameter  $\delta^p$  by the following equation:

$$X_s^p = (\delta^p/\delta)^2 \quad (10)$$

Also, the parameter  $a$ , determined with the polarity and  $X_{LS}$ , is introduced into  $\Phi_G$  as follows:

$$\begin{aligned} \Phi_G &= \Phi_0 (\gamma_L/\gamma_s)^a \\ a &= \left[ \log \left( \frac{\Phi_0 + X_{LS}}{\Phi_0} \right) \right] / \log(\gamma_L/\gamma_s) \\ a &< 0.5 \quad \text{for } d \cos \theta / d\gamma_L < 0 \end{aligned} \quad (11)$$

The  $\Phi_0$  is equal to the bonding efficiency parameter of Kaelble and Uy<sup>22</sup>. Therefore,  $\Phi_G^0$  is expressed by:

$$\Phi_G^0 = [(X_c^d X_s^d)^{0.5} + (X_c^p X_s^p)^{0.5}] (\gamma_c/\gamma_s)^a \quad (12)$$

where  $X_c^d$  is the ratio of  $\gamma_c$  obtained with D liquids and  $\gamma_c$  obtained with P or H liquids<sup>11</sup>. The surface tension  $\gamma_s$  is obtained from equations (8) and (12) as follows:

$$\gamma_s = \gamma_c [(X_c^d X_s^d)^{0.5} + (X_c^p X_s^p)^{0.5}]^{2/(2a-1)} \quad (13)$$

Also, the reversible work of adhesion  $W_a$  is expressed by:

$$W_a = 2\Phi_0 (\gamma_s^{0.5-a} \gamma_L^{0.5+a}) \quad (14)$$

Consequently, the combination of equation (14) and Young–Dupre’s equation (3) leads to:

$$\log(1 + \cos \theta) = -\psi \log(\gamma_L) + \log(2\Phi_0 \gamma_s^{0.5-a}) \quad (15)$$

Using equation (15), the parameter  $a$  is determined with the slope  $\psi = (0.5 - a)$  in the plot of  $\log(1 + \cos \theta)$  versus  $\log(\gamma_L)$  and  $\gamma_c$  is obtained from the value of  $\gamma_L$  at  $\log(1 + \cos \theta) = \log 2$  by extrapolating the straight line.

## EXPERIMENTAL

### Materials

The structure of P(VDF-HFA) used in this study is shown in Figure 2; the HFA contents and the molecular weights of P(VDF-HFA) are shown in Table 1. The molecular weights of P(VDF-HFA) were measured by gel permeation chromatography using a Toso G-HXL column with 0.4 mol% DMF at 40°C. The P(VDF-HFA) films used in contact angle measurements were

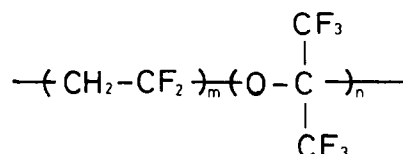


**Figure 2** Structure of P(VDF-HFA)

prepared by coating with 20 wt% THF solution onto poly(ethylene terephthalate) (PET) film using LINTEC Universal Coating system. The P(VDF-HFA) films were dried at 90°C for 60 s, then laminated with the release liner. The P(VDF-HFA) films were then seasoned at  $23 \pm 3^\circ\text{C}$  and  $65 \pm 5\%$  r.h. for 7 days. The films were 30  $\mu\text{m}$  thick in their dry states.

#### Contact angle measurement

The contact angles of P(VDF-HFA) films with various liquids were measured by Kyowa Kaimen Kagaku CA-D type. The 1.5–2.0 mm diameter drops of liquids were prepared with a microsyringe, and they were dropped on the surface of P(VDF-HFA) films at 20°C. The surface tensions  $\gamma_L$  and the polarity  $X_L^p$  of the organic liquids, D, P and H, are shown in Table 2.

## RESULTS

The Zisman plots ( $\cos \theta$  versus  $\gamma_L$ ) for P(VDF-HFA) (HFA content 10.4 mol%) with the organic liquids are shown in Figure 3. The critical surface tensions  $\gamma_c$  of P(VDF-HFA) evaluated by Zisman's linear approximation have various values with varying polarity of liquids. The magnitude of the critical surface tension  $\gamma_c$  for P(VDF-HFA) film increases in the order: D < H < P liquids.

**Table 1** Hexafluoroacetone (HFA) contents and molecular weights of fluorocopolymers

HFA content (mol%)	$M_n$	$M_w$	$M_w/M_n$
6.5	30 000	127 000	4.23
8.3	11 600	57 300	4.94
10.4	35 000	162 000	4.63

liquids. Substituting equation (3) into (2), the relationships between  $1 + \cos \theta$  and  $1/\gamma_L^{0.5}$  are shown in Figure 4. The  $\gamma_c$  values of P(VDF-HFA) evaluated with the  $1 + \cos \theta$  versus  $1/\gamma_L^{0.5}$  plot also have various values with varying polarity of liquids used. The magnitude of  $\gamma_c$  also increases in the order: D < H < P liquids. The straight lines between  $1 + \cos \theta$  and  $1/\gamma_L^{0.5}$  approximated by the method of least squares greatly deviated from the origin. The  $\log(1 + \cos \theta)$  versus  $\log(\gamma_L)$  plots are shown in Figure 5. The order of magnitude of  $\gamma_c$  evaluated with this plot is similar to those on the other plots.

The  $\gamma_c$  values of P(VDF-HFA) films obtained by all the plots, the intercept  $\phi$  of  $1 + \cos \theta$  at  $1/\gamma_L^{0.5} = 0$  in the  $1 + \cos \theta$  versus  $1/\gamma_L^{0.5}$  plot and the slope  $-\psi$  on the  $\log(1 + \cos \theta)$  versus  $\log(\gamma_L)$  plot are shown in Table 3. The  $\gamma_c$  values estimated by the Zisman plot are smaller than those estimated by other plots.  $\phi$  decreases with increasing HFA content in P(VDF-HFA) and it has a minimum with the P liquids. The slope  $-\psi$  decreases

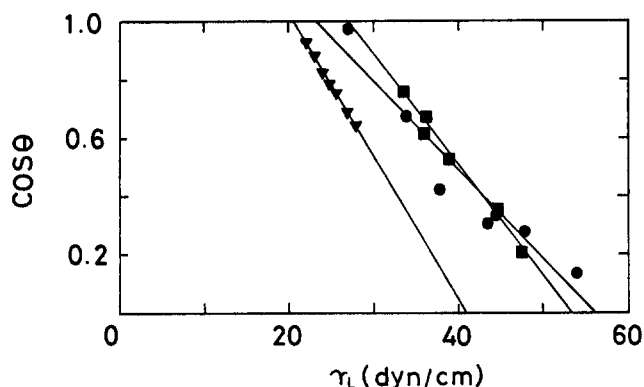


**Figure 3** Zisman plots for P(VDF-HFA) with 10.4 mol% HFA content. ●, H liquids; ▼, D liquids; ■, P liquids

**Table 2** The surface tensions and polarity ( $X_L^p$ ) of liquids at 20°C (in  $\text{dyn cm}^{-1}$ ) from ref. 31

Species	Liquid	$\gamma_L^d$	$\gamma_L^e$	$\gamma_L^f$	$\gamma_L$	$X_L^p$
D	n-Octane	21.8	0	0	21.8	0
	n-Nonane	22.9	0	0	22.9	0
	n-Decane	23.9	0	0	23.9	0
	n-Undecane	24.7	0	0	24.7	0
	n-Dodecane	25.4	0	0	25.4	0
	n-Tetradecane	26.7	0	0	26.7	0
	n-Hexadecane	27.6	0	0	27.6	0
P	1,1,2-Trichloroethane <sup>a</sup>	—	—	—	33.6	—
	Hexachlorobutadiene <sup>a</sup>	35.8	0.2	0	36.0	0.006
	Tetrachloroethane	33.2	3.1	0	36.3	0.085
	1,2-Dibromoethane <sup>a</sup>	—	—	—	38.9	—
	$\alpha$ -Bromonaphthalene	44.4	0.2	0	44.6	0.004
	Tetrabromoethane	44.3	3.2	0	47.5	0.067
H	1-Methoxy-2-propanol <sup>a</sup>	—	—	—	27.1	—
	Dipropylene glycol	29.4	0	4.5	33.9	0.133
	1,3-Butanediol <sup>a,b</sup>	—	—	—	37.8	—
	Polyethyleneglycol	29.9	0.1	13.5	43.5	0.313
	Diethyleneglycol	31.7	0	12.7	44.4	0.286
	Ethyleneglycol	30.1	0	17.8	47.7	0.369
Thiodiglycol	39.2	1.4	13.4	54.0	0.274	

<sup>a</sup>Data from ref. 32

<sup>b</sup>Surface tension of 1,3-butanediol at 25°C

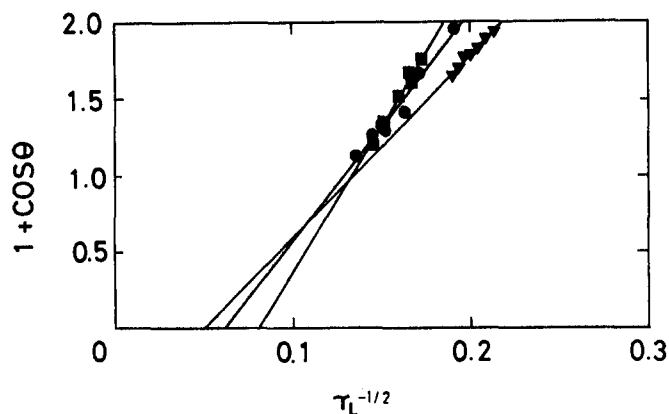


Figure 4 Young-Dupre-Good-Girifalco plots for P(VDF-HFA) with 10.4 mol% HFA content. ●, H liquids; ▼, D liquids; ■, P liquids

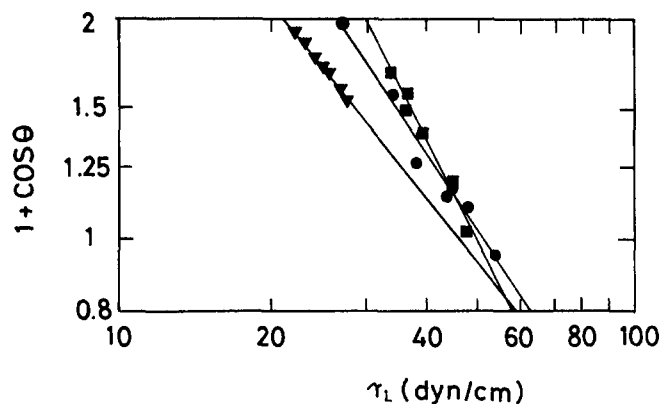


Figure 5 Log(1 + cos θ) versus log(γ<sub>L</sub>) plots for P(VDF-HFA) with 10.4 mol% HFA content. ●, H liquids; ▼, D liquids; ■, P liquids

with increasing HFA content in P(VDF-HFA) and it also has a minimum with the P liquids.

## DISCUSSION

On the Zisman plot, the relationship between  $\cos \theta$  and  $\gamma_L$  displays a favourable straight line when the value of  $\gamma_L$  is in the vicinity of  $\gamma_c$ . On the other hand, it displays a downwardly convex curve<sup>23</sup> when  $\gamma_L$  has a value much larger than  $\gamma_c$ , because a liquid with  $\gamma_L$  much greater than  $\gamma_c$  generally possesses the specific interaction (hydrogen bonding<sup>24</sup>). Gutowski<sup>25</sup> defined the following equation:

$$1 + \cos \theta = 2\Phi_G \left( \frac{\gamma_s}{\gamma_L} \right)^{0.5} \quad (16)$$

Equation (16) is derived from substituting Young-Dupre's equation (3) into Good-Girifalco's equation (2). Gutowski<sup>25</sup> pointed out that the Zisman plot ( $\cos \theta$  versus  $\gamma_L$ ) essentially demonstrated a downwardly convex curve with equation (16).

In this study, the Zisman plot and the critical surface tensions  $\gamma_c$  of P(VDF-HFA) are discussed by use of the intercept  $\phi$  of  $1 + \cos \theta$  at  $1/\gamma_L^{0.5} = 0$  in the  $1 + \cos \theta$  versus  $1/\gamma_L^{0.5}$  plot and the slope  $-\psi$  in the  $\log(1 + \cos \theta)$  versus  $\log(\gamma_L)$  plot. The relationship between  $\cos \theta$  and  $\gamma_L$  can be defined with the  $\phi$  or  $\psi$  by the following equations: from equation (7) and equation (16):

$$\cos \theta = (2 - \phi)(\gamma_c/\gamma_L)^{0.5} + (\phi - 1) \quad (17)$$

from equation (11) and equation (16):

$$\cos \theta = 2\Phi_0(\gamma_s/\gamma_L)^{\psi-1} \quad (18)$$

Therefore, the relationship between  $\cos \theta$  and  $\gamma_L$  obtained using equation (17) (for  $\phi < 2$ ) illustrates a downwardly convex curve. The  $\gamma_c$  values estimated by the Zisman plot and equation (17) are provided as  $\gamma_c^E$  and  $\gamma_c^T$ , respectively. As the polarity  $X_L^P$  of respective liquids in the P and H liquids differ remarkably (Table 2), it is suggested that the  $\Phi_0$  also depends on the liquid. Thus, the relation on the Zisman plot and the  $\gamma_c$  in this study is discussed with equation (17).

As can be seen in Table 3, the parameters  $\phi$  of all P(VDF-HFA) films have negative values. The relationship between  $\cos \theta$  and  $\gamma_L$  for P(VDF-HFA) with 10.4 mol% HFA content, evaluated with the  $\phi$  and  $\gamma_c$  in Table 3, is expressed with equation (17) as follows:

$$\text{for D} \quad \cos \theta = 11.81(\gamma_L)^{-0.5} - 1.59$$

$$\text{for P} \quad \cos \theta = 19.08(\gamma_L)^{-0.5} - 2.53$$

$$\text{for H} \quad \cos \theta = 14.95(\gamma_L)^{-0.5} - 1.92$$

Both the relationship between  $\cos \theta$  and  $\gamma_L$  obtained from equation (17) and the straight line on the Zisman plot expressed by the method of least squares are shown in Figure 6. For the D liquids,  $\gamma_c^E$  is nearly equal to  $\gamma_c^T$ . On the other hand,  $\gamma_c^E$  is obviously smaller than  $\gamma_c^T$  for the P and the H liquids. Also, the relationship between  $\cos \theta$  and  $\gamma_L$  (experimental data) is approximately fitted with the theoretical curve calculated by equation (17). Consequently, we can presume that the Zisman plot is essentially a downwardly convex curve with the P and H liquids having  $\gamma_c \ll \gamma_L$ . This result is consistent with that of Gutowski<sup>25</sup>.

When the liquid contacts the polymer solid, it is known that the orientation of the polar groups<sup>26</sup> and the rearrangement of the side chain of the polymer<sup>10,11</sup> occur near the interface. In this case, the surface tension  $\gamma_s$  of polymer solid and the theoretical surface tension  $\gamma_c^T$  are changed with varying the polarity of the liquids. The polarity  $X_s^P$  and  $\gamma_s$  of P(VDF-HFA) evaluated by the slope  $-\psi$  of the  $\log(1 + \cos \theta)$  versus  $\log(\gamma_L)$  plot are

Table 3 The critical surface tensions  $\gamma_c$  of fluorocopolymers and the constants determined from various plots

Constant	Species	HFA content (mol%)		
		6.5	8.3	10.4
$\gamma_c$ : critical surface tension by Zisman plot	D	21.2	19.9	20.4
	P	27.9	24.4	26.9
$\cos \theta$ versus $\gamma_L$	H	22.7	22.6	23.1
$\gamma_c$ : critical surface tension by (1 + cos θ) versus 1/γ <sub>L</sub> <sup>0.5</sup> plot	D	21.4	20.4	20.8
	P	29.8	27.8	29.2
	H	27.5	25.9	26.2
$\gamma_c$ : critical surface tension by log(1 + cos θ) versus log(γ <sub>L</sub> ) plot	D	21.5	20.6	20.9
	P	30.3	28.5	30.0
	H	28.1	26.0	26.4
$\phi$ : intercept of (1 + cos θ) axis in the plot of (1 + cos θ) versus 1/γ <sub>L</sub> <sup>0.5</sup>	D	-0.07	-0.44	-0.59
	P	-0.88	-0.97	-1.53
	H	-0.41	-0.74	-0.92
(-ψ) = -(0.5 - a): slope (-ψ) in the plot of log(1 + cos θ) versus log(γ <sub>L</sub> )	D	-0.52	-0.63	-0.67
	P	-0.79	-0.82	-1.04
	H	-0.65	-0.73	-0.79

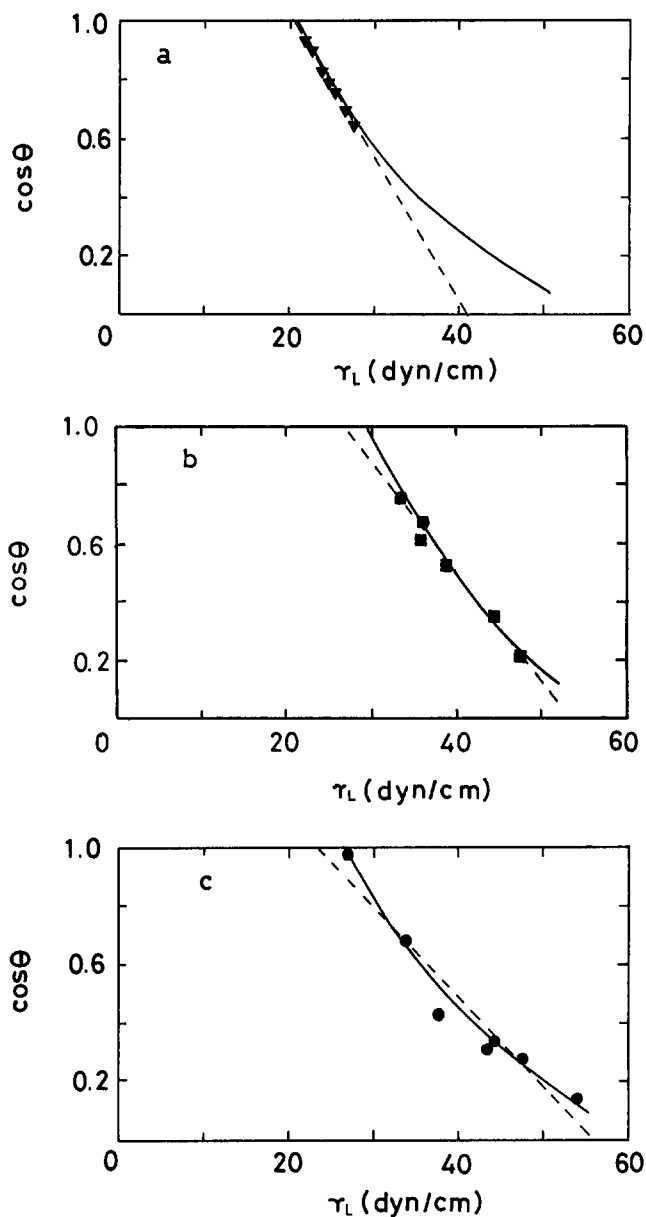


Figure 6 Theoretical curves of  $\cos \theta$  versus  $\gamma_L$  based on the equation  $\cos \theta = (2 - \phi)(\gamma_c/\gamma_L)^{0.5} + (\phi - 1)$ . (a) D liquids; (b) P liquids; (c) H liquids

Table 4 The surface tensions  $\gamma_s$  and the polarity  $X_s^p$  of fluorocopolymers

HFA content (mol%)	$X_s^p$	$\gamma_s^a$		
		D	P	H
6.5	0.055	22.7	32.5	29.7
8.3	0.072	21.9	29.9	26.7
10.4	0.089	22.7	33.6	26.9

<sup>a</sup> $\gamma_s$  is calculated from the equation:

$$\gamma_s = \gamma_c [(X_c^d X_s^d)^{0.5} + (X_c^p X_s^p)^{0.5}]^{2/(2a-1)}$$

shown in Table 4. The  $\gamma_s$  value is close to the  $\gamma_c$  estimated by the  $\log(1 + \cos \theta)$  versus  $\log(\gamma_L)$  plot. Also the  $\gamma_s$  has a maximum for the P liquids. It is suggested that the orientation of the polar group and the rearrangement of the side chain in P(VDF-HFA) take place near the polymer surface in contact with the liquid.

In the polymer blend and the polymer containing plasticizer, surface segregation has occurred as the low surface energy component has been preferentially enriched on the surface of the sample by the difference between the surface energies of components<sup>19,20,27,28</sup>. Patel and co-workers<sup>20</sup> confirmed by X-ray photoelectron spectroscopy that the siloxane blocks having low surface energy in the polystyrene/poly(sulphone-siloxane-sulphone) block copolymer blends are enriched on the surface of blends. We found out that surface segregation occurred in the PEHA/P(VDF-HFA) blends<sup>13,15,16,18</sup>. In a previous paper<sup>18</sup>, it was suggested that the origins of the surface segregation came from the immiscibility of the P(VDF-HFA) and the PEHA and the significantly low surface tension  $\gamma_s$  of P(VDF-HFA). In this paper, the surface segregation for the PEHA/P(VDF-HFA) blends was interpreted with  $\gamma_s$  and miscibility observed by thermophotometry<sup>29,30</sup>. Figure 7 shows the miscibility for the PEHA/P(VDF-HFA) (HFA content 10.4 mol%) blends observed by means of thermophotometry. The blend samples displayed opacity in the range 25–300°C. The opacity for blends of PEHA/P(VDF-HFA) (HFA content 6.5 and 8.3 mol%) was also observed in the temperature range 25–300°C. Thus, it is suggested that the blends of PEHA with P(VDF-HFA) (HFA content 6.5, 8.3 and 10.4 mol%) are remarkably immiscible. The relationships between  $\gamma_s$  obtained by equation (13) and the HFA contents of P(VDF-HFA) are shown in Figure 8. The  $\gamma_s$  values of P(VDF-HFA) (HFA content 8.3 mol%) are smaller than those of P(VDF-HFA) with other contents about 1–4 dyn cm<sup>-1</sup>. Therefore, it is predicted that P(VDF-HFA) with 8.3 mol% HFA content, which has the minimum  $\gamma_s$  value, most easily induced surface segregation.

CONCLUSION

The contact angles of organic liquids on P(VDF-HFA) films were measured. The  $\gamma_c$  values of P(VDF-HFA)

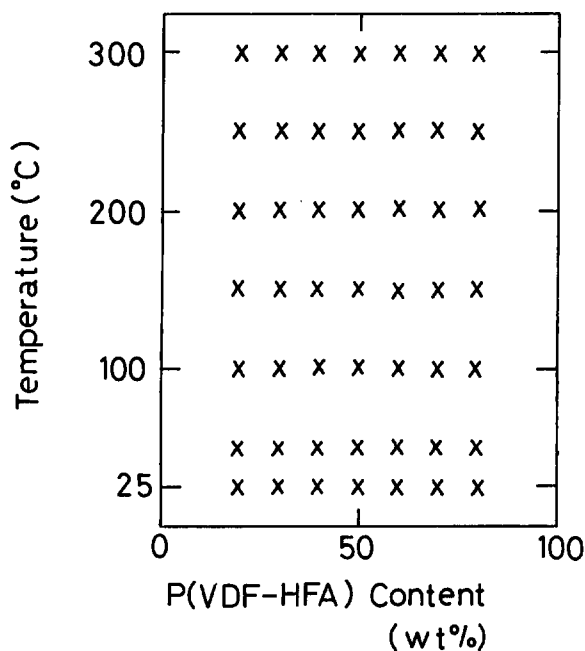


Figure 7 Miscibility in PEHA/P(VDF-HFA) blends (HFA content 10.4 mol%) with visual observation by thermophotometry. The symbol x indicates opacity. Heating rate 5°C min<sup>-1</sup>

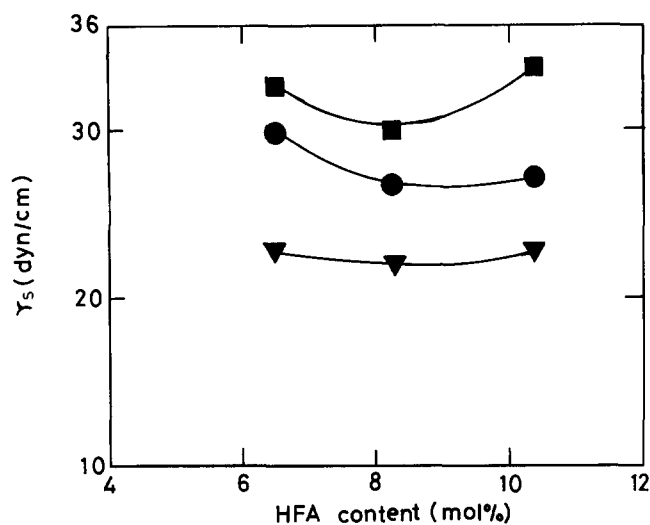


Figure 8 Relationship between the surface tension  $\gamma_s$  and HFA content of P(VDF-HFA).  $\gamma_s$  is calculated using equation (13). ●, H liquids; ▼, D liquids; ■, P liquids

films obtained with the Zisman plot ( $\cos \theta$  versus  $\gamma_L$ ) were smaller than those obtained with either the  $1 + \cos \theta$  versus  $1/\gamma_L^{0.5}$  plot or the  $\log(1 + \cos \theta)$  versus  $\log(\gamma_L)$  plot. It was found that the Zisman plot resulted in essentially a downwardly convex curve. The  $\gamma_s$  evaluated by the  $\log(1 + \cos \theta)$  versus  $\log(\gamma_L)$  plot and equation (13) had a maximum for the P liquids. Thus, we considered that orientation and rearrangement of P(VDF-HFA) occurred. Also, the surface tension of P(VDF-HFA)  $\gamma_s$  revealed a minimum at the HFA content of 8.3 mol%. Therefore, we can expect that the P(VDF-HFA) with 8.3 mol% HFA most easily induced the surface segregation.

#### ACKNOWLEDGEMENTS

The authors express their sincere thanks to Dr T. Saito for valuable theoretical instruction and to Central Glass Co. Ltd for supplying the fluoro-copolymers.

#### REFERENCES

- Miyata, S. and Kobayashi, S. *Gendai Kagaku Zokan* 1988, **8**, 134
- Hasegawa, M. and Akiyama, S. *Polym. J.* 1988, **20**, 471
- Akiyama, S. and Hashimoto, Y. *Bull. Fac. Gen. Educ. Tokyo Univ. Agr. Tech.* 1986, **23**, 79
- Fox, H. W. and Zisman, W. A. *J. Colloid Sci.* 1950, **5**, 514; 1952, **7**, 109; 1952, **7**, 428
- Zisman, W. A. in 'Contact Angle, Wettability and Adhesion', (Ed. F. M. Fowkes), American Chemical Society, Washington, DC, 1964, pp. 1-51
- Girifalco, L. A. and Good, R. J. *J. Phys. Chem.* 1957, **61**, 904; Good, R. J. and Girifalco, L. A. *J. Phys. Chem.* 1960, **64**, 541; Good, R. J. in 'Contact Angle, Wettability and Adhesion', (Ed. F. M. Fowkes), American Chemical Society, Washington DC, 1964, p. 99
- Hata, T., Kitazaki, Y. and Saito, T. *J. Adhesion* 1987, **24**, 177
- Saito, T. *J. Adhesion Soc. Jpn* 1988, **24**, 347
- Saito, T. *J. Adhesion Soc. Jpn* 1988, **24**, 431
- Saito, T. and Kano, Y. *J. Adhesion Soc. Jpn* 1988, **24**, 469
- Kano, Y. and Saito, T. *Setchaku* 1988, **32**, 396
- Akiyama, S., Ushiki, H. and Sugiyama, H. *Rep. Prog. Polym. Phys. Jpn* 1988, **XXXI**, 455
- Kano, Y. and Akiyama, S. *J. Adhesion Soc. Jpn* 1990, **26**, 173
- Akiyama, S., Kawahara, S. and Tsuchiya, A. *Bull. Fac. Gen. Educ. Tokyo Univ. Agr. Tech.* 1989, **26**, 93
- Kano, Y., Ishikura, K. and Akiyama, S. *J. Adhesion Soc. Jpn* 1990, **26**, 252
- Kano, Y., Kamagami, S. and Akiyama, S. *J. Adhesion Soc. Jpn* 1990, **26**, 284
- Jpn Pat. 63-117085 to Central Glass Co., 1985
- Kano, Y. and Akiyama, S. *J. Adhesion Soc. Jpn* 1990, **26**, 367
- Saito, T. 'A Phenomenological Approach to the Reversible Work of Adhesion and the Interfacial Tension', Nippon Setchaku Gakkai, Osaka, 1988, p. 379
- Patel, N. M., Dwight, D. W., Hedrick, J. L., Webster, D. C. and McGrath, J. E. *Macromolecules* 1988, **21**, 2689
- Wu, S. 'Polymer Interface and Adhesion', Marcel Dekker, New York, 1982, p. 105
- Kaelble, D. H. and Uy, K. C. *J. Adhesion* 1970, **2**, 50
- Allan, A. J. G. *J. Polym. Sci.* 1959, **38**, 297
- Wu, S. 'Polymer Interface and Adhesion', Marcel Dekker, New York, 1982, p. 183
- Gutowski, W. *J. Adhesion* 1985, **19**, 29
- Hirasawa, E. and Ishimoto, R. *J. Adhesion Soc. Jpn* 1982, **18**, 247; 1985, **19**, 29
- Inoue, H. *J. Adhesion Soc. Jpn* 1990, **26**, 81
- Miki, T., Kohzai, K. and Yonemura, U. *Polym. Prepr. Jpn* 1990, **38**, 1281
- Akiyama, S. and Kaneko, R. *Kobunshi Ronbunshu* 1974, **31**, 12
- Akiyama, S. and Hasegawa, M. *Bull. Fac. Gen. Educ. Tokyo Univ. Agr. Tech.* 1986, **23**, 79
- Kitazaki, Y. and Hata, T. *J. Adhesion Soc. Jpn* 1972, **8**, 133
- Youzai Handbook, Kodansya, 1976